

Supporting Information

Selective Oxidation of Sacrificial Ethanol over TiO₂-based Photocatalysts during Water Splitting

Haiqiang Lu,^{a,b} Jianghong Zhao,^a Li Li,^a Liming Gong,^{a,b} Jianfeng Zheng,^a Lexi Zhang,^{a,b} Zhijian Wang,^{a,b} Jian Zhang,^{a,b} Zhenping Zhu^{*,a}

This supporting information contains experimental methods and Figures S1-S7.

Experimental methods

Preparation and characterization of TiO₂ materials

TiO₂ structure modulation was performed using a calcination method with commercial TiO₂ powder (P25, Degussa) as a starting material. The powder had an anatase/rutile ratio of about 80/20 and a specific surface area of about 50 m²/g. A typical calcination was carried out in a muffle furnace in air at 700 (for 2 h), 750 (for 2 h), 800 (for 8 h) and 900 °C (for 8 h).

Rutile TiO₂ nanotubes were synthesized using a TiO₂-NaOH-ethanol ternary reaction system under hydrothermal conditions. The detailed experimental information was described elsewhere.¹ TiO₂ nanoparticles were synthesized using an alcoholysis-based sol-gel method similar to the method reported in reference.² Briefly, 10 mL of tetrabutyl orthotitanate and 2.5 mL of acetylacetone (as a stabilizer) were dissolved in 20 mL of anhydrous ethanol, and then magnetically stirred for 60 min. After ageing for 3 days, the obtained sol was dried at 60 °C for 7 d to obtain a gel. The TiO₂ gel was finally calcinated at 600 °C for 5 h.

Filling pure rutile TiO₂ nanotubes with paraffin liquid

Pure rutile TiO₂ nanotubes were synthesized using a TiO₂-NaOH-ethanol ternary reaction system under hydrothermal conditions. Liquid paraffin was encapsulated inside rutile TiO₂ nanotubes using the experimental method. Here, 1 g of the TiO₂ nanotubes was first vacuumed for 30 min to remove the original air inside them. The tubes were then filled with 2 mL liquid paraffin. The paraffin left outside the tubes was dislodged by deionized water, and the paraffin-filled tubes obtained were dispersed in aqueous ethanol solution for reaction testing and in-situ Pt loading.

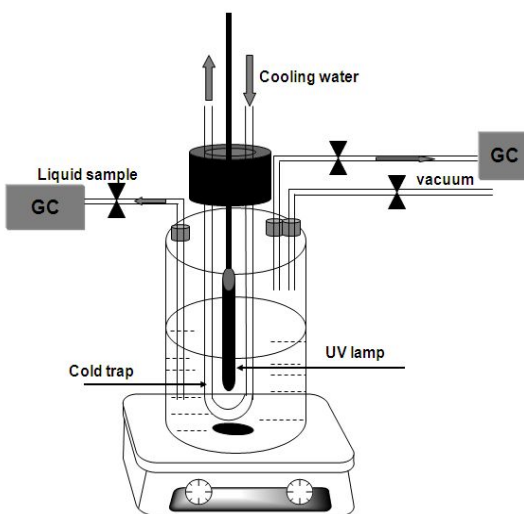
Characterization of catalysts

The phase structure of the TiO₂-based photocatalyst was examined by X-ray diffraction (XRD) using a BRUKER D8 Advance X-ray diffractometer with Cu K α radiation ($\lambda=0.15406$ nm) operating at 40 kV. TEM images were obtained on a JEM-2010 electron microscope operated at 200 kV. All samples were

prepared by suspension in ethanol and drop-cast onto a carbon-coated copper TEM grid. The UV–Vis absorption spectra were recorded on a Shimadzu UV 3600 UV-Vis-NIR spectrophotometer. Raman measurements were performed on a Jobin–Yvon HR-800 Raman system, using the 514 nm line of an Ar laser as the excitation source. Specific surface areas were measured by the BET method, employing N₂ adsorption at 77 K and using a Tristar-3000 apparatus.

Photocatalysis tests

Photocatalytic experiments were performed using a closed system with an inner-irradiation-type Pyrex reactor, as shown in right figure. A 300-W high pressure Hg lamp was plunged into a quartz immersion well cooled by water. All the photocatalytic tests were carried out using 1 g of photocatalyst and 200 mL of 30 vol% aqueous ethanol solution. An appropriate amount (1% Pt) of chloroplatinic acid, H₂PtCl₆·6H₂O, was added to the solution. The suspension was magnetically stirred under vacuum for 10 min to remove the original air, and the UV lamp was turned on to allow the reaction to proceed. During the reaction, both gaseous and liquid products were sampled and analyzed using gas chromatography (GC). The structures of the products were confirmed by comparison with standard samples and by GC-MS (Shimadzu; GCMS-QP2010 Plus).



The reactor for photocatalytic water-splitting. During the reaction, both gaseous and liquid products were sampled and analyzed using gas chromatography (GC). The structures of the products were confirmed by comparison with standard samples and by GC-MS (Shimadzu; GCMS-QP2010 Plus).

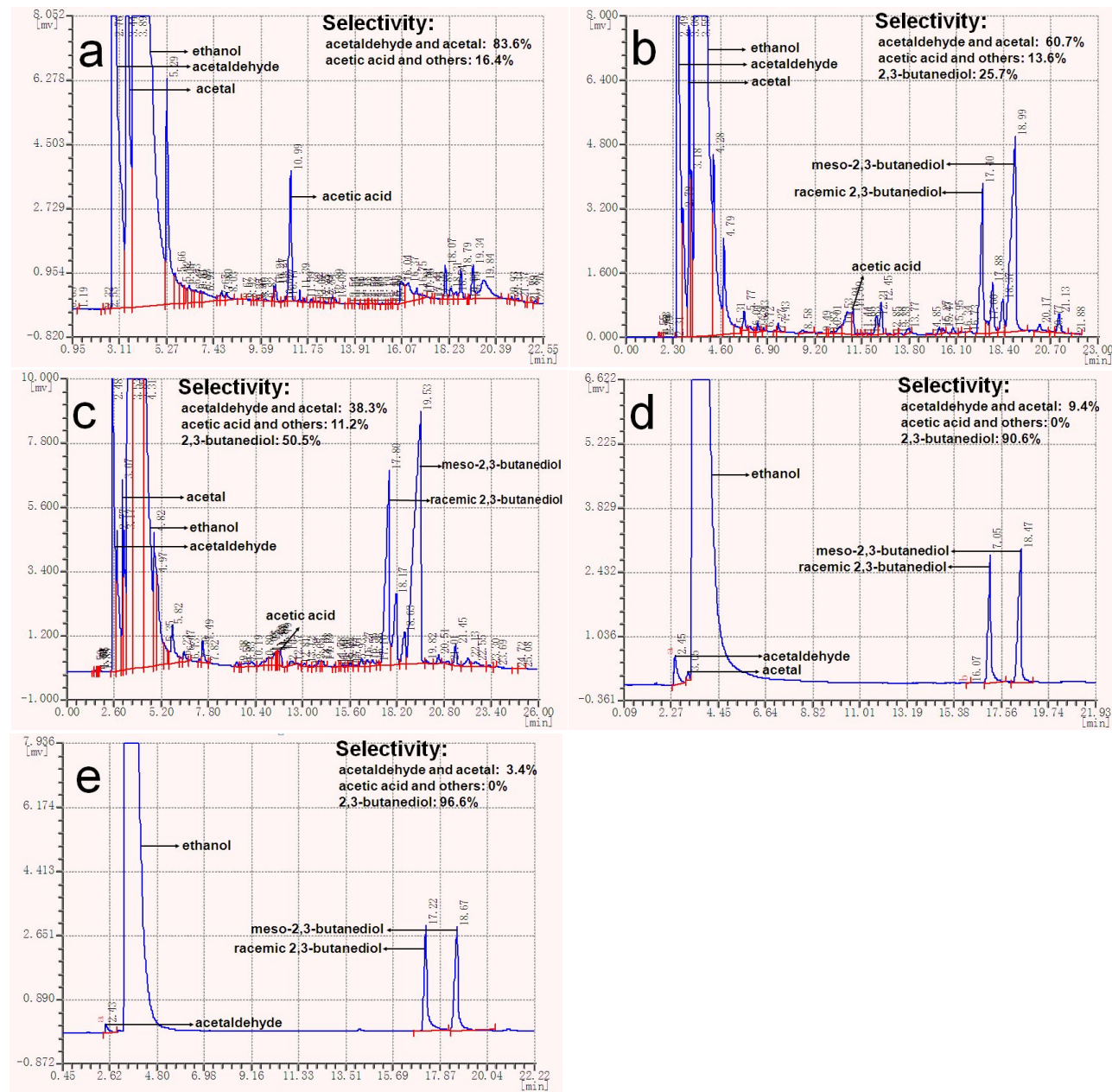


Figure S1. Gas chromatogram of the liquid products obtained from a UV irradiation of 30 vol% deaerated aqueous ethanol solution, with Pt-loaded TiO₂ catalysts. (a) original P25, (b) calcinated at 700 °C for 2 h, (c) calcinated at 750 °C for 2 h, (d) calcinated at 800 °C for 8 h, (e) calcinated at 900 °C for 8 h.

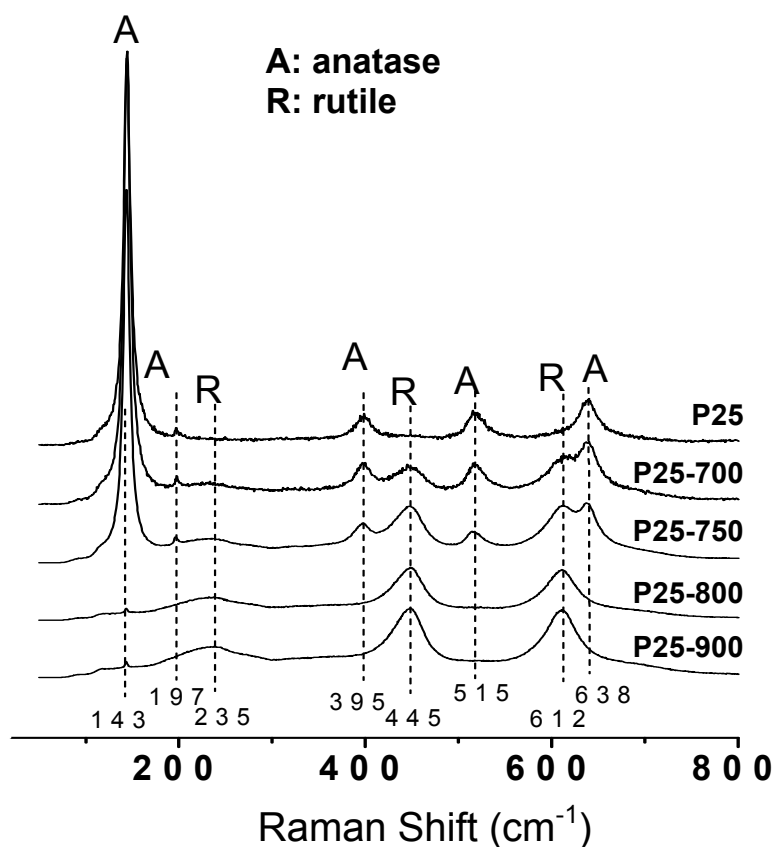


Figure S2. Raman spectra of the samples obtained by the calcination of P25 TiO₂ at different temperatures. The anatase phase(A) shows major Raman bands at 144, 197, 395, 515, and 638 cm⁻¹. These bands can be attributed to the five Raman-active modes of anatase phase with the symmetries of Eg, Eg, A1g, B1g, and Eg, respectively. The typical Raman bands due to rutile phase(R) appear at 143(superimposed with the 144 cm⁻¹ band due to anatase phase), 235, 445, and 612 cm⁻¹, which can be ascribed to the B1g, two-phonon scattering, Eg, and A1g modes of rutile phase, respectively.³

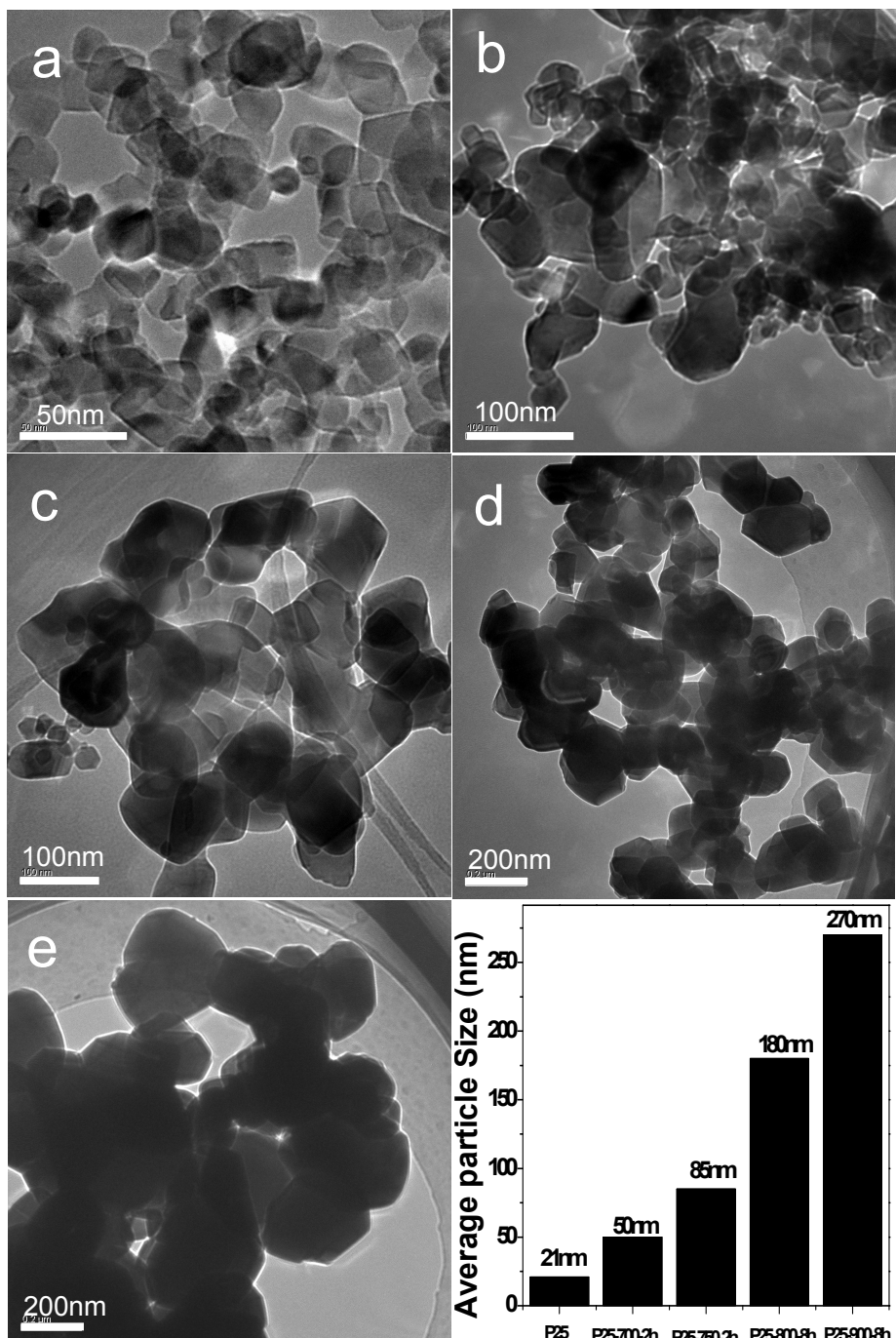


Figure S3. TEM images of TiO_2 samples. (a) Original P25, (b) calcinated at 700 °C for 2 h, (c) calcinated at 750 °C for 2 h, (d) calcinated at 800 °C for 8 h, (e) calcinated at 900 °C for 8 h. (f) Size dependence of calcination temperature, which shows that the aggregation of TiO_2 particles is visible upon the calcinations.

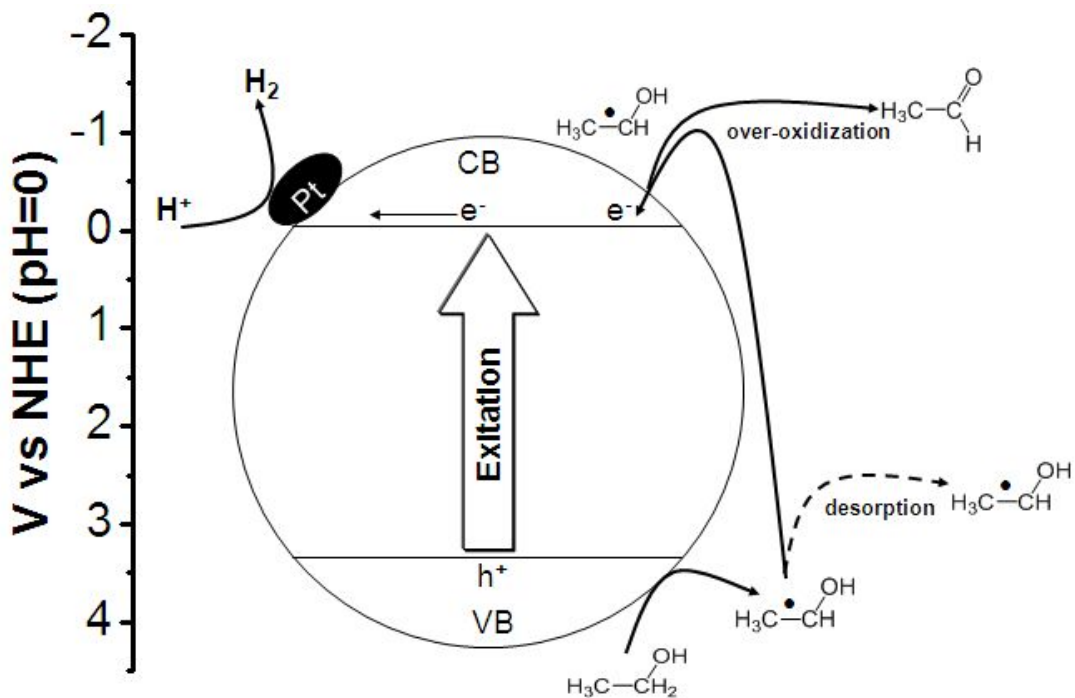


Figure S4. A schematic of the previous explanation to the failure of TiO_2 for the catalysis of alcohol coupling reaction, in which the conduction band was presumed to be too positive so as a alcohol radical would inject its electron into the conduction band and thus be over-oxidized to aldehyde.⁴

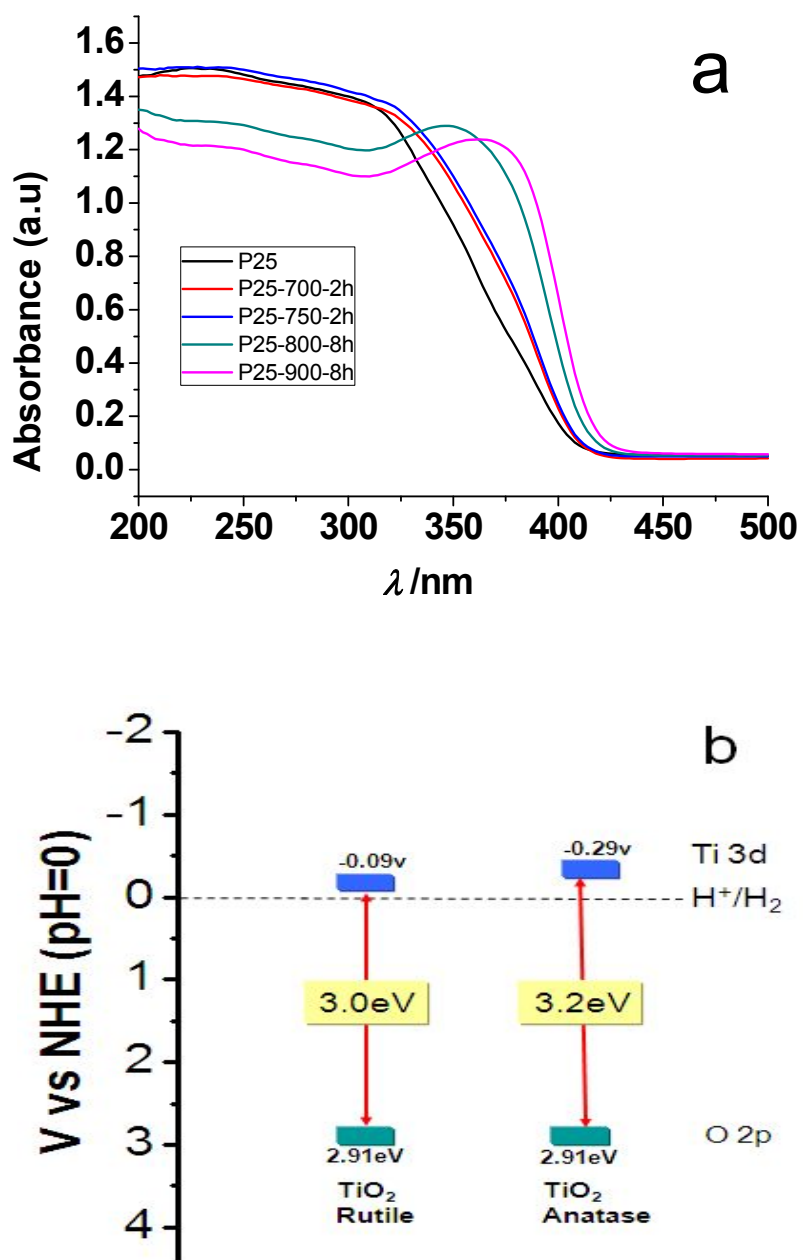


Figure S5. (a) UV-vis absorption spectra of the TiO_2 samples. (b) A schematic of the band structure of TiO_2 with different phase structures, rutile and anatase,⁵ in which the conduction band of the rutile is more positive than the conduction band of anatase.

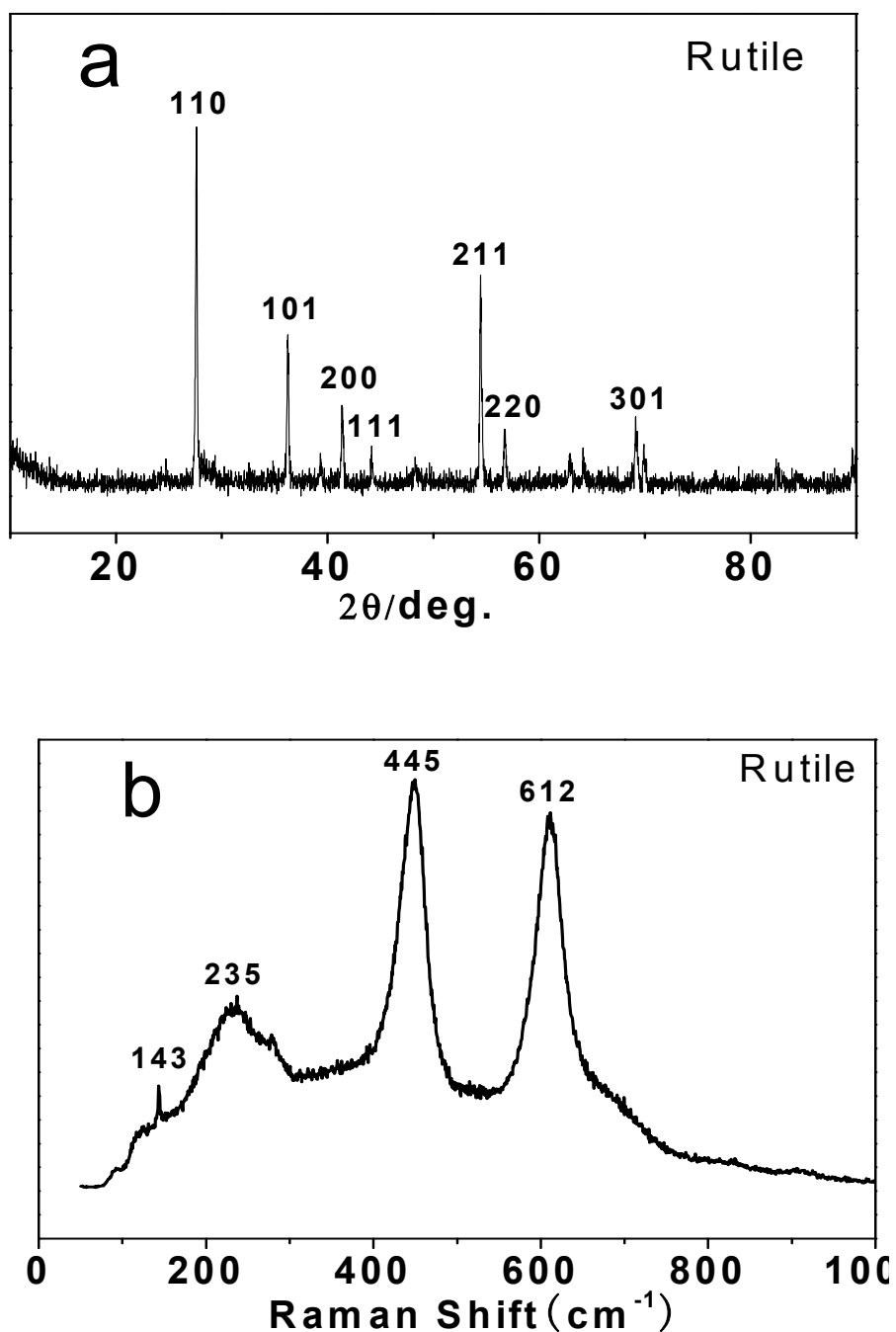


Figure S6. (a) XRD pattern and (b) Raman spectrum of the TiO_2 nanotubes. They indicate that the nanotubes exhibit a pure rutile phase structure.

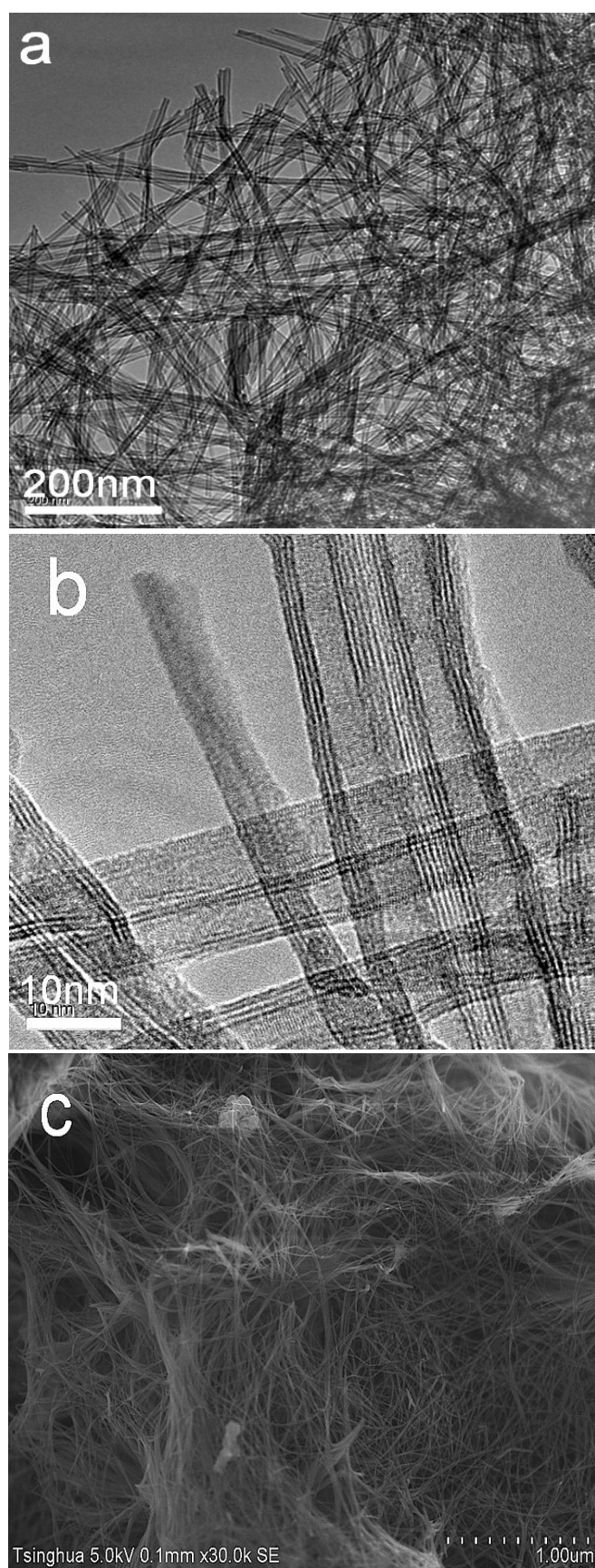


Figure S7. (a) TEM, (b) HR-TEM, and (c) FE-SEM images of the rutile TiO_2 nanotubes.

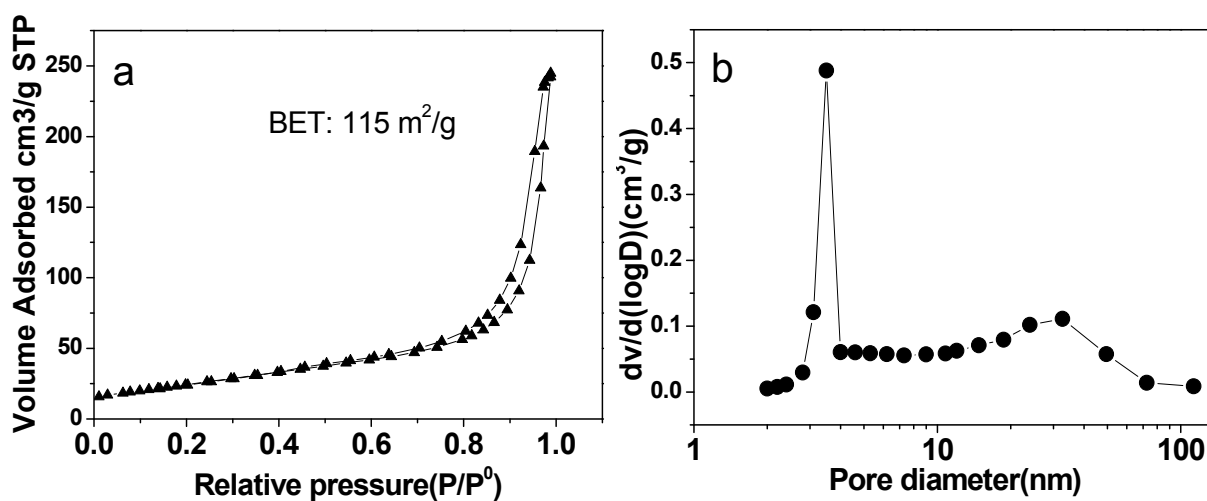


Figure S8. (a) N₂ adsorption/desorption isotherms of the rutile TiO₂ nanotubes. (b) The pore size distribution of the rutile TiO₂ nanotubes.

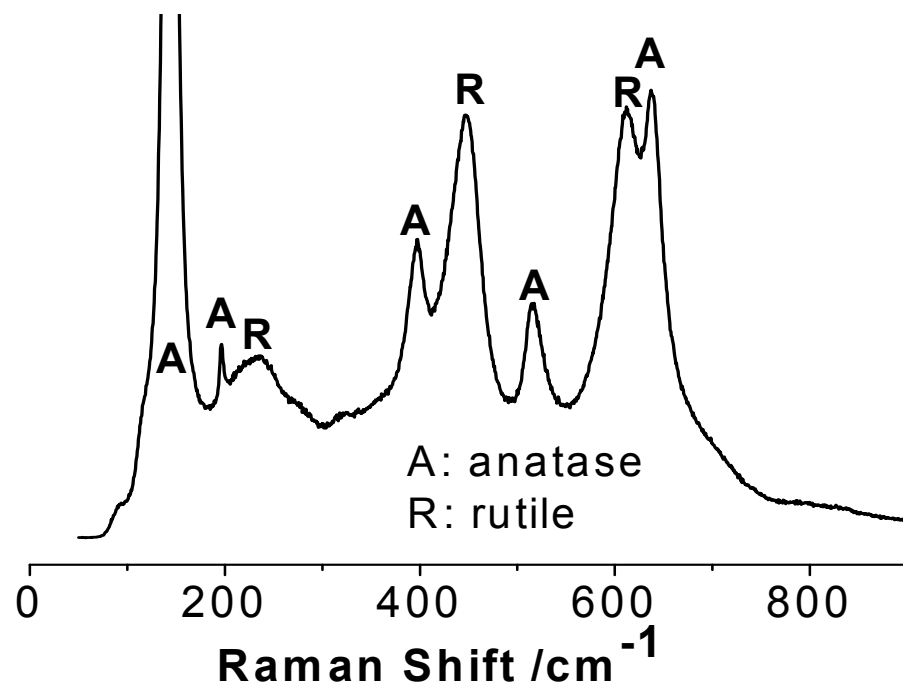


Figure S9. Raman spectrum of the TiO₂ nanoparticles synthesized by an alcoholysis-based sol-gel method. Detailed attributions of the Raman peaks are similar to Figure S2.

References

- (1) Yan, J.; Feng, S.; Lu, H.; Wang, J.; Zheng, J.; Zhao, J.; Li, L.; Zhu, Z. *Mater. Sci. Eng.: B* **2010**, 172, 114.
- (2) Lu, H.; Zhang, L.; Xing, W.; Wang, H.; Xu, N. *Mater. Chem. Phys.* **2005**, 94, 322.
- (3) Zhang, J.; Li, M.; Feng, Z.; Chen, J.; Li, C. *J. Phys. Chem. B* **2006**, 110, 927
- (4) Müller, B.; Majoni, S.; Memming, R.; Meissner, D. *J. Phys. Chem. B* **1997**, 101, 2501.
- (5) Leung, D.; Fu, X.; Wang, C.; Ni, M.; Leung, M.; Wang, X. *ChemSusChem* **2010**, 3, 681.